Eur. Phys. J. D **37**, 83–92 (2006)
DOI: 10.1140/epjd/e2005-00266-6

THE EUROPEAN PHYSICAL JOURNAL D

Capture of slow antiprotons by helium atoms

J. Révai[1] and N. Shevchenko[2,a]

[1] Research Institute for Particle and Nuclear Physics, P.O.B. 49, 1525 Budapest, Hungary
[2] Joint Institute for Nuclear Research, Dubna 141980, Russia

Received 15 July 2005
Published online 4 October 2005 –

Abstract. A consistent quantum mechanical calculation of partial cross-sections leading to different final states of antiprotonic helium atom was performed. For the four-body scattering wave function, corresponding to the initial state, as well as for the antiprotonic helium wave function, appearing in the final state, adiabatic approximations were used. Further, symmetric and non-symmetric effective charge (SEC, NEC) approximations were introduced for the two-electron wave functions in the field of the two fixed charges of the He nucleus and the antiproton. Calculations were carried out for a wide range of antiprotonic helium states and incident energies of the antiproton below the first ionization threshold of the He atom. The origin of the rich low-energy structure of certain cross-sections is discussed in detail.

PACS. 36.10.-k Exotic atoms and molecules (containing mesons, muons, and other unusual particles) – 25.43.+t Antiproton-induced reactions – 34.90.+q Other topics in atomic and molecular collision processes and interactions

1 Introduction

One of the most impressive success stories of the last decade in few-body physics is the high precision experimental and theoretical studies of long lived states in antiprotonic helium (for an overview see [1]). While the energy levels have been both measured and calculated to an extreme precision, allowing even an improvement of numerical values of fundamental physical constants, some other relevant properties of these states were studied with considerably less accuracy. Among these is the formation probability of different metastable states, characterized by total angular momentum J and "vibrational" quantum number v, in the capture reaction

$$\bar{p} + {}^4\mathrm{He} \longrightarrow ({}^4\mathrm{He}^+\,\bar{p})_{Jv} + e^-. \tag{1}$$

The existing calculations of the capture rates of slow antiprotons in He [2–4] are based on classical or semiclassical approaches and they mainly address the reproduction of the overall fraction (3%) of delayed annihilation events. Recent experimental results from the ASACUSA project [5], however, yield some information on individual populations of different metastable states, and our aim is to perform a fully quantum mechanical calculation of the formation probability of different states in the capture reaction.

The exact solution of the quantum mechanical four-body problem, underlying the reaction (1) is far beyond the scope of this work, and probably also of presently available calculational possibilities. Still, we want to make a full quantum mechanical, though approximate, calculation of the above process. Full is meant in the sense that all degrees of freedom are taken explicitly into account, all the wave functions we use, are true four-body states.

2 Calculation method

The partial cross-section, leading to a specified final state (J, v) of the antiprotonic helium can be written as

$$\sigma_{Jv} = 2\,(2\pi)^4\,\frac{K_f}{K_i}\,\mu_i\,\mu_f \int d\Omega_{\mathbf{K}_f}\,\left|\left\langle \Phi^f_{Jv,\mathbf{K}_f}|V_f|\,\Psi^i_{\mathrm{He},\mathbf{K}_i}\right\rangle\right|^2 \tag{2}$$

where $\Psi^i_{\mathrm{He},\mathbf{K}_i}$ is the exact 4-body scattering wave function corresponding to the initial state

$$\Phi^i_{\mathrm{He},\,\mathbf{K}_i}(\mathbf{r}_1,\mathbf{r}_2,\mathbf{R}) = \Phi_{\mathrm{He}}(\mathbf{r}_1,\mathbf{r}_2)\,\frac{1}{(2\pi)^{3/2}}\,e^{i\mathbf{K}_i\mathbf{R}}, \tag{3}$$

while the final state $\Phi^f_{Jv,\,\mathbf{K}_f}$ is taken in the form

$$\Phi^f_{Jv,\,\mathbf{K}_f}(\boldsymbol{\rho}_1,\boldsymbol{\rho}_2,\mathbf{R}) = \Phi_{Jv}(\boldsymbol{\rho}_1,\mathbf{R})\,\frac{1}{(2\pi)^{3/2}}\,e^{i\mathbf{K}_f\boldsymbol{\rho}_2}. \tag{4}$$

Here $\mathbf{r}_i$ are the vectors pointing from the helium nucleus to the ith electron, $\mathbf{R}$ is the vector between He and $\bar{p}$, and

[a] e-mail: shev@thsun1.jinr.ru

$\boldsymbol{\rho}_i$ are the Jacobian coordinates of the electrons, measured from the He$-\bar{p}$ center of mass:

$$\mathbf{r}_i = \boldsymbol{\rho}_i + \alpha\,\mathbf{R}; \qquad \alpha = \frac{m_{\bar{p}}}{m_{\bar{p}} + m_{\mathrm{He}}}, \tag{5}$$

while μ_i and μ_f are the reduced masses in initial and final channels, respectively. In equation (3) $\Phi_{\mathrm{He}}(\mathbf{r}_1, \mathbf{r}_2)$ denotes the He ground state wave function, while in equation (4) $\Phi_{Jv}(\boldsymbol{\rho}_1, \mathbf{R})$ is the antiprotonic helium final state, for which we used a Born-Oppenheimer form [6,7]:

$$\Phi_{Jv}(\boldsymbol{\rho}, \mathbf{R}) = \frac{\chi_{Jv}(R)}{R}\, Y_{JM}(\hat{R})\; \varphi_{1\sigma}^{(2,-1)}(\boldsymbol{\rho}; \mathbf{R}) \tag{6}$$

where $\varphi_{1\sigma}^{(Z_1,Z_2)}(\boldsymbol{\rho}; \mathbf{R})$ is a two-center wave function, describing the electron (ground state) motion in the field of two charges (Z_1, Z_2), separated by a fixed distance R:

$$\left(-\frac{1}{2}\Delta_{\mathbf{r}} + \frac{Z_1}{r} + \frac{Z_2}{|\mathbf{r}-\mathbf{R}|}\right)\; \varphi_{1\sigma}^{(Z_1,Z_2)}(\mathbf{r}; \mathbf{R}) = \varepsilon_{1\sigma}^{(Z_1,Z_2)}(R)\varphi_{1\sigma}^{(Z_1,Z_2)}(\mathbf{r}; \mathbf{R}) \tag{7}$$

while $\chi_{Jv}(R)$ is the heavy-particle relative motion wave function, corresponding to $(^4\mathrm{He}\,\bar{p}\,e^-)$ angular momentum J and "vibrational" quantum number v:

$$\left(-\frac{1}{2\mu}\left[\frac{d^2}{dR^2} - \frac{J(J+1)}{R^2}\right] - \frac{2}{R} + \varepsilon_{1\sigma}^{(2,-1)}(R) - E_{J,v}\right)\chi_{Jv}(R) = 0, \tag{8}$$

μ being the He $-\,\bar{p}$ reduced mass. Since in the following we shall deal only with 1σ two-center ground states, the index 1σ will be omitted throughout the paper.

The transition potential in equation (2) is obviously the interaction of the emitted electron (#2) with the rest of the system:

$$V_f = -\frac{2}{\mathbf{r}_2} + \frac{1}{|\mathbf{r}_2 - \mathbf{R}|} + \frac{1}{|\mathbf{r}_1 - \mathbf{r}_2|}. \tag{9}$$

The electron anti-symmetrization is accounted for by taking an $r_1 \Longleftrightarrow r_2$ symmetric initial state wave function $(S = 0)$ and the factor 2 in front of the cross-section (2), reflecting the indistinguishability of emitted particles [8].

The general expression (2) for the cross-section, leading to a specific state (J, v) can be rewritten in terms of matrix elements between angular momentum eigenstates as

$$\sigma_{Jv} = 2\,(2\pi)^4\,\frac{K_f}{K_i}\,\mu_i\,\mu_f \sum_{J_t,l}(2J_t+1)\,|M_{J,l}^{J_t}|^2 \tag{10}$$

with

$$M_{J,l}^{J_t} = \langle [\Phi_{Jv}(\boldsymbol{\rho}_1, \mathbf{R})\phi_{K_f,l}(\boldsymbol{\rho}_2)]_{M_t}^{J_t} \,|\, V_f \,|\, \Psi_{\mathrm{He},K_i}^{i\,J_t,M_t}(\boldsymbol{\rho}_1, \boldsymbol{\rho}_2, \mathbf{R})\,\rangle, \tag{11}$$

where $[\ ]_M^J$ stands for vector coupling, $\Psi_{\mathrm{He},K_i}^{iJ_t,M_t}$ is the exact scattering wave function with total angular momentum J_t, corresponding to the initial state

$$[\Phi_{\mathrm{He}}^{J=0}(\mathbf{r}_1, \mathbf{r}_2)\,\phi_{K_i,J_t}(\mathbf{R})]_{M_t}^{J_t}$$

and $\phi_{K_i,l}(\mathbf{r})$ denotes free states with definite angular momentum

$$\phi_{K,l}(\mathbf{r}) = \sqrt{\frac{2}{\pi}}\, j_l(Kr) Y_{lm}(\hat{r}).$$

It can be seen from equations (10, 11), that a given antiprotonic helium final state (J, v) can be formed from different total angular momentum states, depending on the orbital momentum l, carried away by the emitted electron.

The simplest way of approximate evaluation of equation (2) or (10) is to use Born approximation, replacing the exact scattering wave function $\Psi_{\mathrm{He},\mathbf{K}_i}^{i}$ by its asymptotic form $\Phi_{\mathrm{He},\mathbf{K}_i}^{i}$ from equation (3). In order to get an idea of the feasibility of such a "full" (including all degrees of freedom) calculation we evaluated the cross-sections σ_{Jv} in Born approximation in a wide range of quantum numbers (J, v). For the He ground state wave function in this case we used the simplest variational form

$$\Phi_{\mathrm{He}}(\mathbf{r}_1, \mathbf{r}_2) = N\,\exp\left(-\sigma(r_1 + r_2)\right) \tag{12}$$

with $\sigma = 27/16$ taken from book [9]. In spite of the known poor quality of the Born approximation for slow collisions, due to the realistic final state wave function, we hoped to get some information at least about the relative population probabilities of different final states. These expectations were not confirmed, the Born cross-sections turned to be orders of magnitude away from the more realistic ones. The detailed results of the Born calculation can be found in [10].

There are two basic drawbacks of the Born approximation for slow collisions and long-range forces:

— the antiproton "feels" the interaction from the He atom, it approaches, therefore, its wave function in the form of a plane wave has to be modified,
— the He electrons also "feel" the approaching antiproton, the polarization of their wave functions has to be taken into account.

To meet these requirements we used an adiabatic, Born-Oppenheimer type approximation for the wave function Ψ^i:

$$\Psi_{\mathrm{He},\mathbf{K}_i}^{i} \approx \Phi_{\mathrm{He}}(\mathbf{r}_1, \mathbf{r}_2; \mathbf{R})\,\chi_{\mathbf{K}_i}(\mathbf{R}), \tag{13}$$

where $\Phi_{\mathrm{He}}(\mathbf{r}_1, \mathbf{r}_2; \mathbf{R})$ is the ground state wave function of the He atom in the presence of a negative unit charge (the antiproton) at a distance R from the He nucleus:

$$\mathcal{H}_{\mathrm{He},\bar{p}}(R)\,\Phi_{\mathrm{He}}(\mathbf{r}_1, \mathbf{r}_2; \mathbf{R}) = \varepsilon(R)\,\Phi_{\mathrm{He}}(\mathbf{r}_1, \mathbf{r}_2; \mathbf{R}), \tag{14}$$

$$\mathcal{H}_{\mathrm{He},\bar{p}}(R) = -\frac{1}{2}\Delta_{\mathbf{r}_1} - \frac{1}{2}\Delta_{\mathbf{r}_2} - \frac{2}{r_1} - \frac{2}{r_2} + \frac{1}{|\mathbf{r}_1 - \mathbf{r}_2|} + \frac{1}{|\mathbf{r}_1 - \mathbf{R}|} + \frac{1}{|\mathbf{r}_2 - \mathbf{R}|};$$

and $\chi_{\mathbf{K}_i}(\mathbf{R})$ is the antiproton scattering wave function in the adiabatic He $-\,\bar{p}$ potential:

$$V_{\mathrm{He}-\bar{p}}(R) = -\frac{2}{R} + \varepsilon(R). \quad (15)$$

$$\left(-\frac{1}{2\mu}\Delta_{\mathbf{R}} + V_{\mathrm{He}-\bar{p}}(R)\right)\,\chi_{\mathbf{K}_i}(\mathbf{R}) = \frac{K_i^2}{2\mu}\,\chi_{\mathbf{K}_i}(\mathbf{R}). \quad (16)$$

In this approach the most difficult task is the solution of equation (14), the determination of the wave function of two interacting electrons in the field of two fixed charges. Instead of performing a cumbersome variational calculation, as e.g. in [11,12], we follow an approximation scheme proposed by Briggs, Greenland, and Solov'ev (BGS) [13], according to which the solution of equation (14) can be sought in the form of two single-electron two-center wave functions:

$$\Phi_{\mathrm{He}}(\mathbf{r}_1,\mathbf{r}_2;\mathbf{R}) \;\approx\; \varphi^{(Z_{11},Z_{12})}(\mathbf{r}_1;\mathbf{R})\,\varphi^{(Z_{21},Z_{22})}(\mathbf{r}_2;\mathbf{R}) \quad (17)$$

with

$$\left(-\frac{1}{2}\Delta_{\mathbf{r}} + \frac{Z_{i1}}{r} + \frac{Z_{i2}}{|\mathbf{r}-\mathbf{R}|}\right)\,\varphi^{(Z_{i1},Z_{i2})}(\mathbf{r}_1;\mathbf{R}) = \varepsilon^{(Z_{i1},Z_{i2})}(R)\,\varphi^{(Z_{i1},Z_{i2})}(\mathbf{r}_1;\mathbf{R}) \quad (18)$$

and the $\varepsilon(R)$ of equations (14,15) is

$$\varepsilon(R) = \varepsilon^{(Z_{11},Z_{12})}(R) + \varepsilon^{(Z_{21},Z_{22})}(R). \quad (19)$$

In this construction the effect of the electron-electron interaction $|\mathbf{r}_1-\mathbf{r}_2|^{-1}$ in equation (14) is approximated by suitable choice of the effective charges $(Z_{11}, Z_{12}, Z_{21}, Z_{22})$.

BGS suggest to fix the effective charges "seen" by the first electron, Z_{11} and Z_{12}, at the real charges of He and $\bar{p}$, while those for the second one, Z_{21} and Z_{22}, can be obtained from the requirement, that in the two limiting cases $R\to 0$ and $R\to\infty$, the ground state energies of H^- ion and He atom should be reproduced:

$$\varepsilon(R\to 0) = E_{gs}(\mathrm{H}^-), \quad \varepsilon(R\to\infty) = E_{gs}(\mathrm{He}). \quad (20)$$

The conditions (20) are fulfilled for

$$Z_{11} = 2.0, \qquad Z_{12} = -1.0,$$
$$Z_{21} = 1.3444, \qquad Z_{22} = -1.1095. \quad (21)$$

For intermediate R–s $\varepsilon(R)$ is given by (19).

As for He wave function, the two electrons in this case are treated in a non-symmetric way, and the wave function has to be symmetrized explicitly:

$$\Phi_{\mathrm{He}}(\mathbf{r}_1,\mathbf{r}_2;\mathbf{R}) = N(R)\left[\varphi^{(Z_{11},Z_{12})}(\mathbf{r}_1;\mathbf{R})\,\varphi^{(Z_{21},Z_{22})}(\mathbf{r}_2;\mathbf{R}) + \varphi^{(Z_{11},Z_{12})}(\mathbf{r}_2;\mathbf{R})\,\varphi^{(Z_{21},Z_{22})}(\mathbf{r}_1;\mathbf{R})\right]. \quad (22)$$

There is, however, a more symmetric realization of the BGS idea: starting with the plausible requirement, that the two electrons should "see" identical effective charges: $Z_{11} = Z_{21}$, $Z_{22} = Z_{12}$ we still can impose the conditions (20) for $R\to 0$ and $R\to\infty$, only in this case the $\varepsilon(R)$ will be the sum of two equal single-particle energies:

$$\varepsilon(R) = 2\varepsilon^{(Z_{11},Z_{22})}(R).$$

For this case we get

$$Z_{11} = 1.704, \qquad Z_{22} = -0.9776. \quad (23)$$

The $\varepsilon(R)$ in this case is very similar to the previous one, maybe a little closer to the "quasi-exact" variational curve. In this second case — for brevity let us call it SEC (Symmetric Effective Charge), in contrast to the NEC (Non-symmetric Effective Charge) case — the wave function is simply

$$\Phi_{\mathrm{He}}(\mathbf{r}_1,\mathbf{r}_2;\mathbf{R}) \;=\; \varphi^{(Z_{11},Z_{22})}(\mathbf{r}_1;\mathbf{R})\,\varphi^{(Z_{11},Z_{22})}(\mathbf{r}_2;\mathbf{R}). \quad (24)$$

The differences between electronic energies $\varepsilon(R)$ for the NEC, SEC and variational calculations (performed by Ahlrichs et al. [11] and Gibbs [12]) are shown in Figure 1. It is seen that both cases reproduces the variational results remarkably well, while SEC is practically indistinguishable from the more recent of them [12].

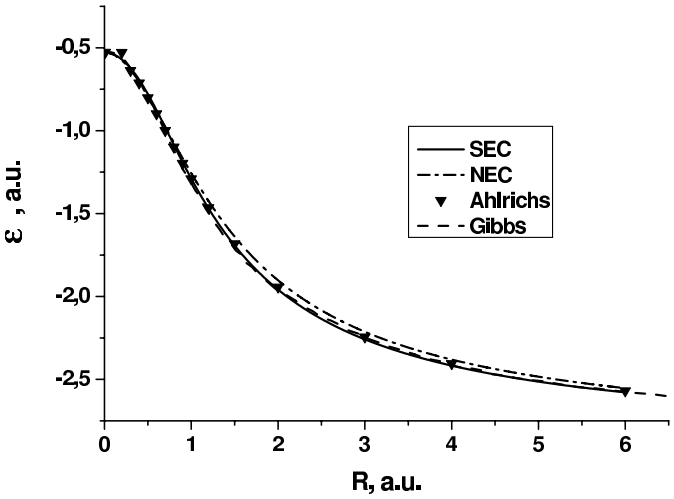

Fig. 1. Electronic energies $\varepsilon(R)$ for the NEC, SEC and variational cases.

For both choices (22) and (24) the definite total angular momentum wave function corresponding to (13) can be written as

$$\Psi^{iJ_tM_t}_{\mathrm{He},K_i}(\mathbf{r_1},\mathbf{r_2},\mathbf{R}) = \Phi_{\mathrm{He}}(\mathbf{r_1},\mathbf{r_2};\mathbf{R})\frac{\chi^{J_t}_{K_i}(R)}{K_iR}Y_{J_t,M_t}(\hat{R}), \quad (25)$$

since the 1σ ground state two-center functions $\varphi(\mathbf{r};\mathbf{R})$ do not carry any total angular momentum: they are eigenfunctions of $\hat{J}^2 = (\hat{l}_{\mathbf{r}} + \hat{L}_{\mathbf{R}})^2$ with zero eigenvalue, even if they are not eigenfunctions of $\hat{l}^2_{\mathbf{r}}$ and $\hat{L}^2_{\mathbf{R}}$ separately. The function $\chi^{J_t}_{K_i}(R)$ satisfies the equation

$$\left[\frac{d^2}{dR^2} - 2\mu\mathsf{V}_{J_t}(R) + K_i^2\right]\,\chi^{J_t}_{K_i}(R) \;=\; 0 \quad (26)$$

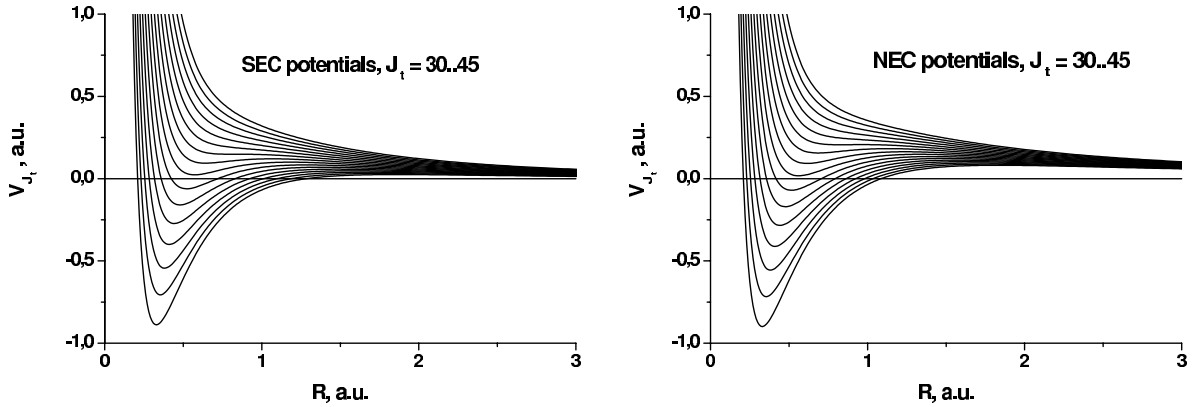

Fig. 2. Effective $\mathrm{He}-\bar{p}$ potentials $\mathsf{V}_{J_t}(R)$ for different J_t values ($J_t = 30$ corresponds to the lowest curve, $J_t = 45$ – to the highest one).

with the effective $\mathrm{He}-\bar{p}$ potential

$$\mathsf{V}_{J_t}(R) = \frac{J_t(J_t+1)}{2\mu R^2} + V_{\mathrm{He}-\bar{p}}(R). \tag{27}$$

To solve equation (26) numerically, first, the asymptotic form of $\chi^{J_t}_{K_i}(R)$ has to be clarified. The asymptotic behavior of the 1σ two-center energies can be written as

$$\varepsilon^{(Z_1,Z_2)}(R) \underset{R\to\infty}{\longrightarrow} -\frac{Z_1^2}{2} - \frac{Z_2}{R} + \mathcal{O}(R^{-4}) \tag{28}$$

and thus using equations (15) and (19) we get

$$V_{\mathrm{He}-\bar{p}}(R) \underset{R\to\infty}{\longrightarrow} -\frac{Z_{11}^2 + Z_{21}^2}{2} - \frac{2 + Z_{12} + Z_{22}}{R} + \mathcal{O}(R^{-4}) \tag{29}$$

Dropping the irrelevant constant term from (29) we see, that asymptotically it corresponds to a Coulomb interaction with effective charge $Z_{as} = -(2 + Z_{12} + Z_{22})$. From the actual values of Z_{12} and Z_{22} (21) and (23) we can conclude, that NEC corresponds to a weak repulsion, while SEC — to an even weaker attraction. In reality, of course, there is no $1/R$ term in the asymptotic $\mathrm{He}-\bar{p}$ interaction, since the He atom is neutral.

It has to be noted, that in spite of the closeness of the NEC and SEC electron energies in Figure 1, when we include the centrifugal term, the depth of the minima and the height of the potential barriers differ significantly (see Fig. 2) and this fact strongly influences the low energy capture cross-sections.

According to (29), equation (26) has to be solved with the asymptotic condition

$$\chi^{J_t}_{K_i}(R) \underset{R\to\infty}{\longrightarrow} \cos\delta_{J_t}(K_i) F_{J_t}(\eta, K_i R) + \sin\delta_{J_t}(K_i) G_{J_t}(\eta, K_i R), \tag{30}$$

where F_{J_t} and G_{J_t} are the regular and irregular Coulomb wave functions, with Sommerfeld-parameter

$$\eta = \frac{Z_{as}\mu}{K_i} \tag{31}$$

and $\delta_{J_t}(K_i)$ is the phase shift caused by the non-Coulombic part of the potential. After the numerical solution of equation (26) with boundary conditions (30) the matrix elements (11) entering the formula (10) for the cross-sections can be calculated by numerical integration.

3 Results and discussion

We start the discussion of our results by the remark, that the expression (11) for the matrix element $M^{J_t}_{J,l}$ in our adiabatic approximation can be rewritten as

$$M^{J_t}_{J,l} \sim \int \chi_{Jv}(R) S_l(R; K_f) \chi^{J_t}_{K_i}(R) dR, \tag{32}$$

where $\chi_{Jv}(R)$ and $\chi^{J_t}_{K_i}(R)$ are the $\mathrm{He}-\bar{p}$ relative motion wave functions, introduced in equations (8) and (25), respectively, while $S_l(R; K_f)$ contains "all the rest": the three potentials (9) integrated over electron wave functions and coordinates, angular variables of $\mathbf{R}$ and summations over intermediate quantum numbers. This representation is useful, since it turns out, that the basic dependence of the matrix elements on the quantum numbers and incident energy is contained in the two χ functions, while $S_l(R; K_f)$ weakly and smoothly depends on its arguments with a significant decrease with increasing l — the orbital momentum of the emitted electron. For a few selected cases the three functions in the integrand of equation (32) are shown in Figure 3. This feature of $S_l(R; K_f)$ allows the interpretation of equation (32) as a matrix element of antiproton transition from the initial state $\chi^{J_t}_{K_i}(R)$ into a final state $\chi_{Jv}(R)$ under the action of the effective potential $S_l(R; K_f)$.

We have calculated the capture cross-sections leading to different final states for antiproton energies below the first ionization threshold $E_{lab} = 30.8$ eV. The overall energy dependence of the NEC and SEC cross-sections $\sigma_{Jv}(E)$ is shown in Figures 4 and 5 for a few quantum numbers from the region of expected largest capture probability. All cross-sections are measured in units of a_0^2, a_0 being the atomic length unit. The main features of these curves can be summarized as follows.

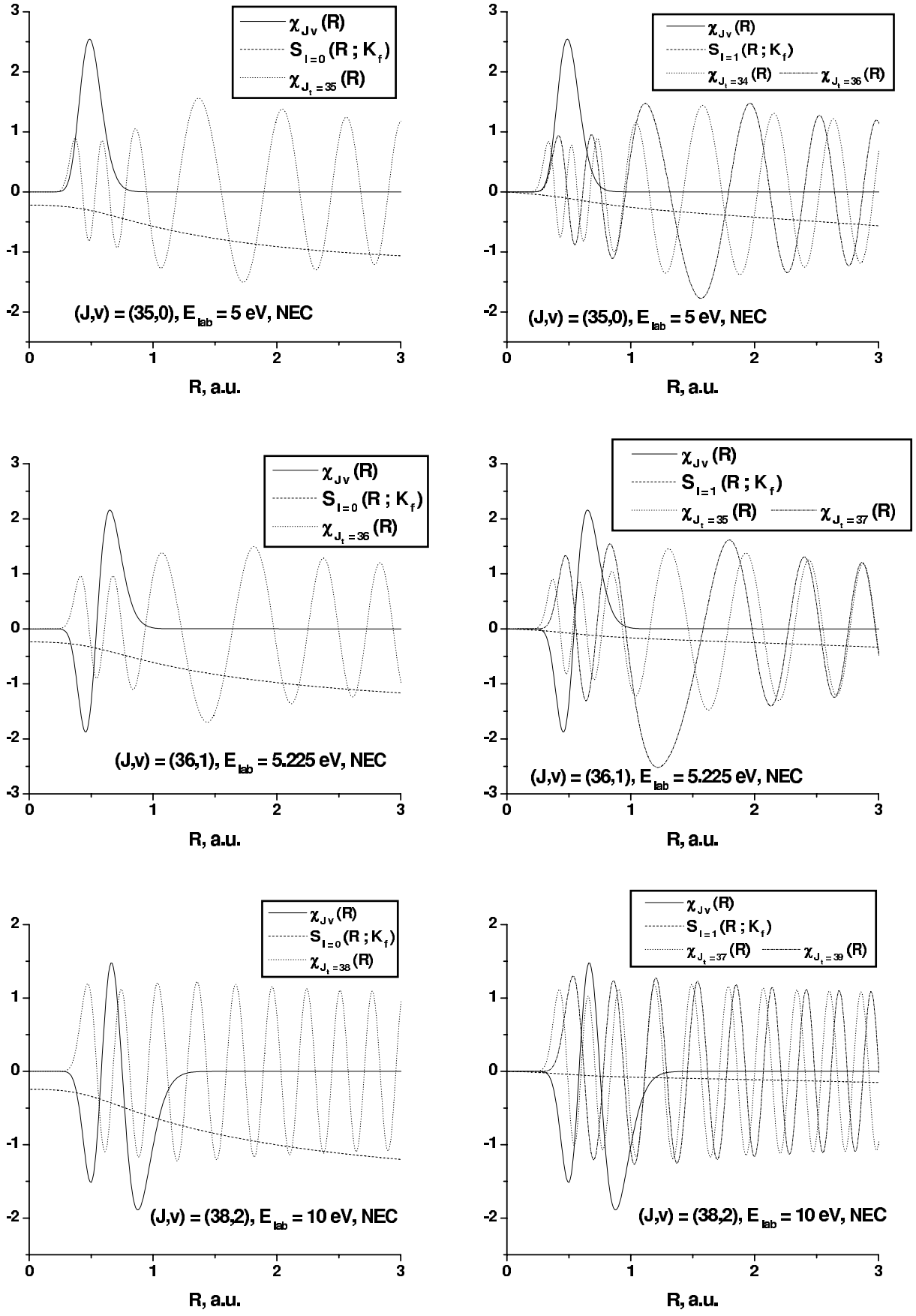

Fig. 3. Functions χ_{Jv}, $\chi^{J_t}_{K_i}$ and S_l for different sets of parameters.

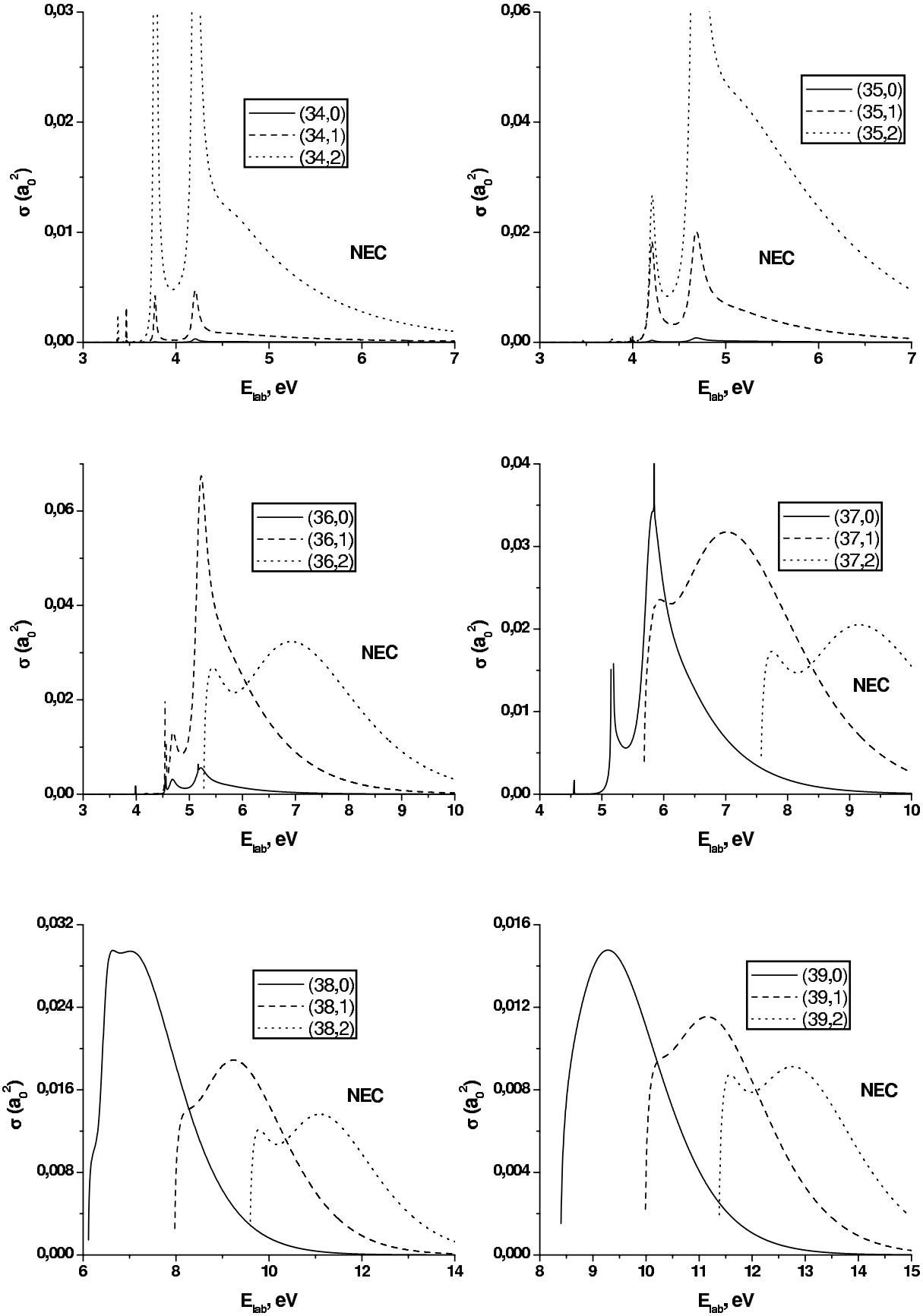

Fig. 4. Energy dependence of the cross-sections for some (J, v) states, NEC case.

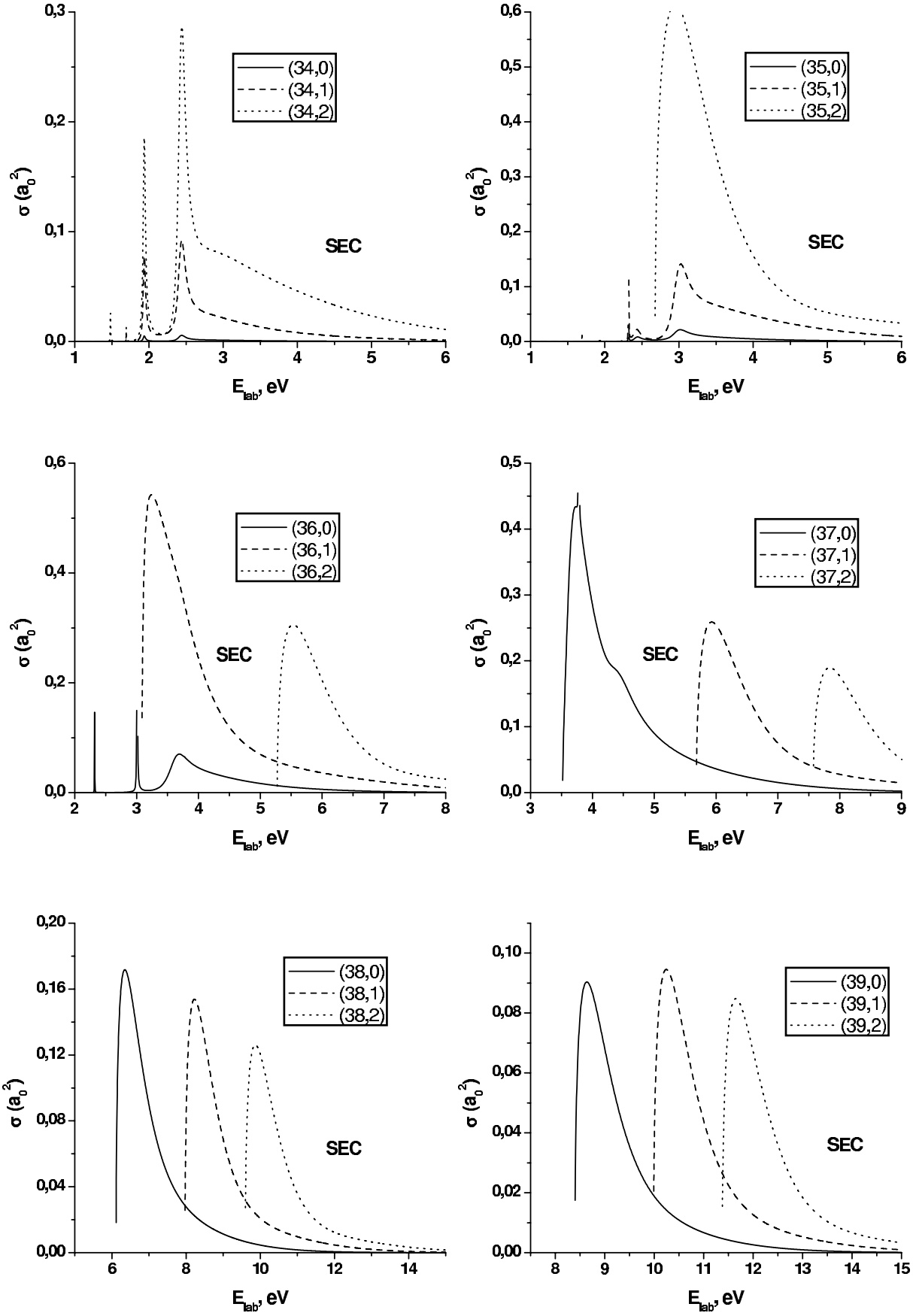

Fig. 5. Energy dependence of the cross-sections for some (J, v) states, SEC case.

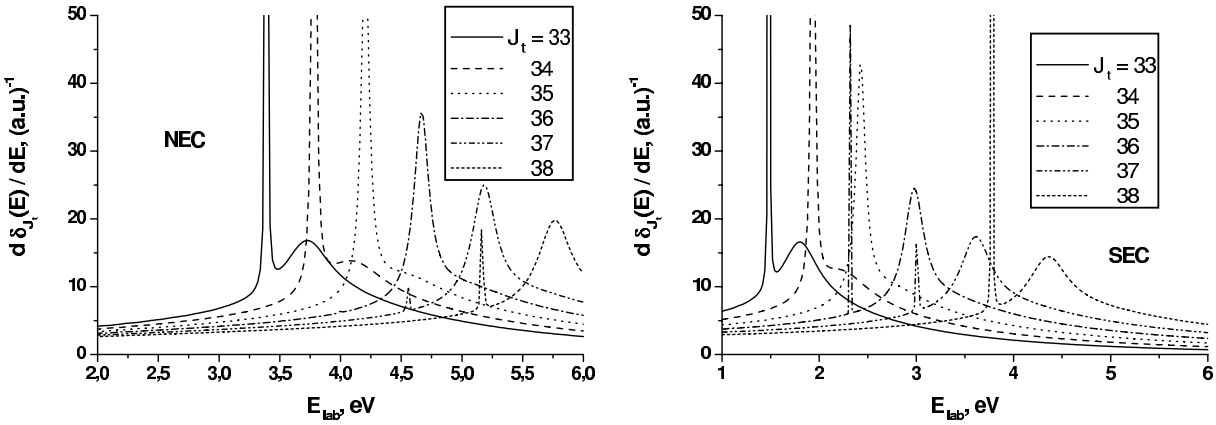

Fig. 6. Time delays for different values of total angular momentum J_t, NEC and SEC cases.

Obviously, final states with energy below the He atom ground state energy (-2.9036 a.u.) have a positive Q value, so they can be reached for arbitrary low antiproton energy. For example, in Figures 4 and 5 there are such states: with $(J = 34, v = 0, 1, 2), (J = 35, v = 0, 1)$, and $(J = 36, v = 0)$. States with higher energy can be excited only above their threshold energies; the steep rise of the cross-sections above these thresholds can be clearly seen.

Another remarkable feature of certain cross-sections is their rich low energy structure. This is due to the repulsive barriers of the effective potentials V_{J_t} for $J_t \leq 38 - 39$, as seen in Figure 2. These barriers, in general, strongly suppress the penetration of $\chi^{J_t}_{K_i}(R)$ into the interior region, thus reducing the sub-barrier cross-sections. For certain sub-barrier energies, however, there are quasi-stationary states in these potentials, when the interior wave function has a large amplitude, leading to sharp resonances in the cross-sections. In order to clarify the origin of these peaks, we looked at the energy dependence of the phase shifts δ_{J_t} of equation (30). In Figure 6 we plotted the quantity $d\delta_{J_t}(E)/dE$ — the so-called time delay — which for isolated resonances is very similar to the more familiar Breit-Wigner cross-section curve. It can be seen, that for all angular momenta J_t for which the potential has a barrier, there is a narrow resonance which is correlated with a corresponding peak in the capture cross-section. A given cross-section curve may contain several of these peaks, corresponding to different J_t and l values contributing to formation of a given final state, according to the sum in equation (10). In general, it is interesting to note, that in contrast to a common belief, the sum of equation (10) is not dominated by the s-electron emission $(J = J_t, l = 0)$ term, the p-electrons practically always, while the d-electrons in certain cases contribute significantly. The reason for this may be, that the decrease of $S_l(R; K_f)$ with growing l could be "compensated" by the possibility of lower J_t values, for which the effective potentials contain less repulsion, thus allowing more penetration of $\chi^{J_t}_{K_i}$ into the interior region.

The $d\delta_{J_t}(E)/dE$ plots apart from the narrow peaks corresponding to quasi-stationary states, show another, much broader peak, in some cases superposed on the narrow one. This one is connected with specific behavior of elastic scattering when the energy is close to the potential maximum; it is called "orbiting" [14].

The behavior of the incident antiproton wave function $\chi_{K_i}(R)$ for different energy-regimes with respect to the barrier maximum are illustrated in Figure 7.

Final states with higher J, for which the relevant effective potentials have no barrier show a simple energy dependence: a steep rise above the threshold and then an exponential decay for higher energies. The exponential fall of the cross-sections for increasing energies is characteristic for both barrier-possessing and barrier-less potentials and is due to increasingly rapid oscillations of $\chi^{J_t}_{K_i}(R)$ in the interior region which reduce the value of the integral in equation (32).

The quantum number dependence of certain cross-sections is shown in Figure 8 for some above-barrier energies, where such a comparison makes sense.

4 Conclusions

To our knowledge, this is the first fully quantum mechanical calculation of the process (1), with all degrees of freedom taken explicitly into account. The adiabatic wave functions used both for initial and final states seem to be reasonably realistic. The results show, that quantum mechanical treatment is really necessary, especially in the low-energy region, where barrier penetration and resonance effects are essential. The energy dependence of the calculated cross-sections shows, that the different final states (J, v) are excited with a large probability in a relatively narrow window of the incident antiproton energy. In principle, this property could be used for selective excitation of certain states. On the other hand, the strong energy dependence of the cross-sections prevents us from making statements about the experimentally observable population numbers of different states since the initial energy distribution of the antiprotons before the capture is unknown. Even if this distribution was known, the observed and calculated population numbers could deviate due to collisional (or other) de-excitation of states in the

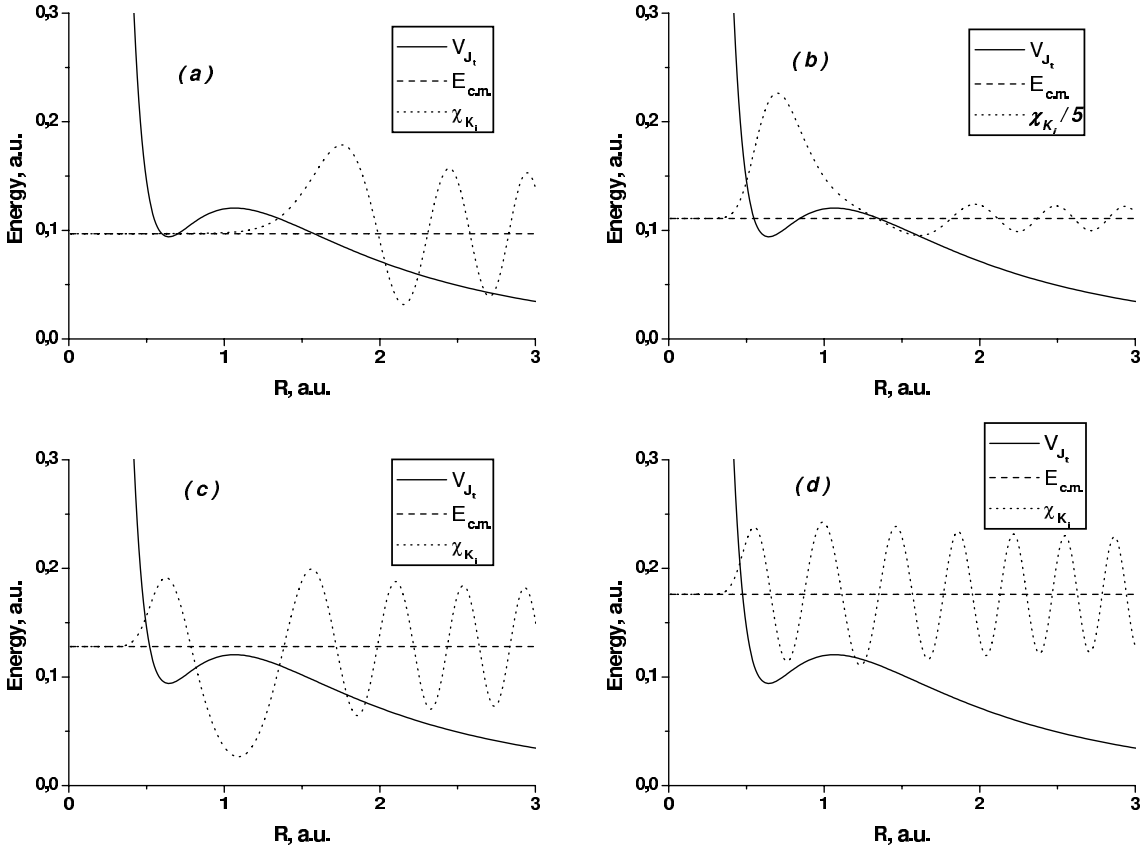

Fig. 7. Incident antiproton wave functions (in arbitrary units) with their potentials. The incident energies (in CM, the baselines for the wave function plots) are chosen to represent different cases with respect to barrier maxima. (a) Sub-barrier non-resonant energy; (b) sub-barrier resonant energy; (c) "orbiting": energy close to the potential maximum; (d) above-barrier energy.

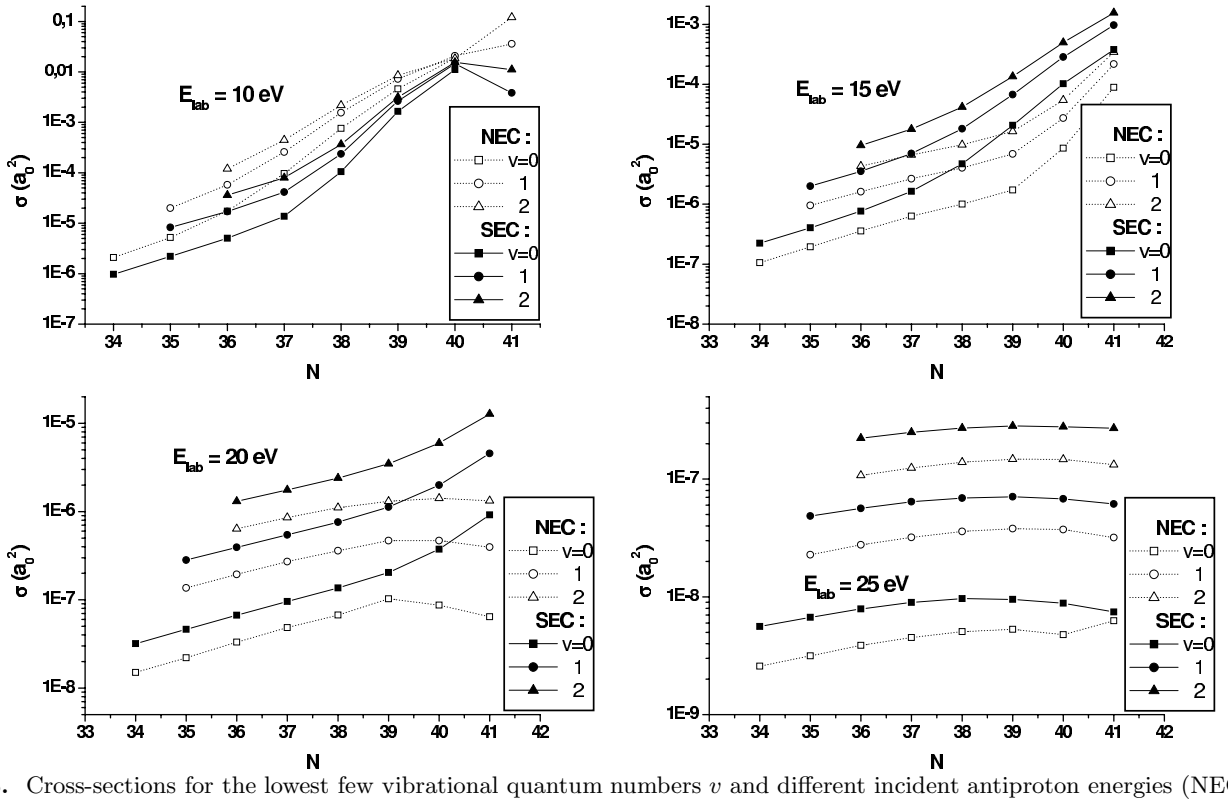

Fig. 8. Cross-sections for the lowest few vibrational quantum numbers v and different incident antiproton energies (NEC and SEC calculations) plotted against the principal quantum number $N = J + v + 1$.

time interval between the capture and the measurement. Nevertheless, we plan to make calculation of primary populations taking some trial energy distributions for the antiprotons.

In the discussion of our results we deliberately did not take a stand concerning the NEC and SEC approximations. In general, the structure of both cross-sections (energy- and quantum number dependence) is similar, however, SEC gives considerably larger cross-sections, probably due to the somewhat larger attraction of the SEC effective potentials. We personally think, that SEC is physically more realistic, and the coincidence of SEC's electronic energies with those of recent variational calculation [12] can be seen as some confirmation for this point of view.

One of the authors (JR) acknowledges the support from OTKA grants T037991 and T042671, while (NVS) is grateful for the hospitality extended to her in the Research Institute for Particle and Nuclear Physics, where a significant part of the work has been done. The authors wish to thank A.T. Kruppa for providing them with one of the necessary computer codes.

References

1. T. Yamazaki et al., Phys. Rep. **366**, 183 (2002)
2. G.A. Korenman, Hyper. Interact. **101-102**, 81 (1996)
3. G.Ya. Korenman, Nucl. Phys. A **692**, 145c (2001)
4. J.S. Cohen, Phys. Rev. A **62**, 022512 (2000)
5. M. Hori et al., Phys. Rev. Lett. **89**, 093401 (2002)
6. I. Shimamura, Phys. Rev. A **46**, 3776 (1992)
7. J. Révai, A.T. Kruppa, Phys. Rev. A **57**, 174 (1998)
8. H. Ekstein, Phys. Rev. **101**, 880 (1956)
9. H.A. Bethe, E.E. Salpeter, *Quantum mechanics of one- and two-electron atoms* (Springer Verlag, Berlin-Göttingen-Heidelberg 1957)
10. J. Révai, N.V. Shevchenko, Preprint `arXiv:physics/0310153` (2003)
11. R. Ahlrichs, O. Dumbrajs, H. Pilkuhn, Z. Phys. A **306**, 297 (1982)
12. W.R. Gibbs, Phys. Rev. A **56**, 3553 (1997)
13. J.S. Briggs, P.T. Greenland, E.A. Solov'ev, J. Phys. B **32**, 197 (1999)
14. R.G. Newton, *Scattering Theory of Waves and Particles* (Springer Verlag, New-York, Heidelberg, Berlin, 1982), p. 600